

Fast-Particle-Driven Alfvénic Modes in a Reversed Field Pinch

J. J. Koliner,* C. B. Forest, J. S. Sarff, J. K. Anderson, D. Liu, M. D. Nornberg, and J. Waksman
Physics Department, University of Wisconsin-Madison, Madison, Wisconsin 53706, USA

L. Lin, D. L. Brower, and W. X. Ding
Department of Physics and Astronomy, University of California Los Angeles, Los Angeles, California 90095-7099, USA

D. A. Spong

Oak Ridge National Laboratory, Oak Ridge, Tennessee 37831-6169, USA

(Received 24 March 2012; revised manuscript received 19 June 2012; published 13 September 2012)

Alfvénic modes are observed due to neutral beam injection for the first time in a reversed field pinch plasma. Modeling of the beam deposition and slowing down shows that the velocity and radial localization are high. This allows instability drive from inverse Landau damping of a bump-on-tail in the parallel distribution function or from free energy in the fast ion density gradient. Mode switching from a lower frequency toroidal mode number $n = 5$ mode that scales with beam injection velocity to a higher frequency $n = 4$ mode with Alfvénic scaling is observed.

DOI: [10.1103/PhysRevLett.109.115003](https://doi.org/10.1103/PhysRevLett.109.115003)

PACS numbers: 52.35.Qz, 52.35.Bj

Alfvén waves that couple to fast particle dynamics comprise a rich field of study within plasma physics. In magnetic confinement of plasmas, neutral beams, rf heating, and fusion reactions can all generate a population of fast ions with some characteristic velocity comparable to the Alfvén speed ($v_A = \frac{B}{\sqrt{\mu_0 m_i n_i}}$), leading to a strong wave-particle interaction that both excites instabilities and causes these particles to be lost or redistributed [1]. In space, shocks propagating at the Alfvén speed can accelerate ions well above the thermal velocity of background media [2]. As magnetic confinement progresses toward fusion and designs for spacecraft that fly further and faster are explored, these resonant interactions become increasingly relevant as both a tool and a challenge to overcome. Of particular interest in the magnetic confinement fusion community are toroidicity-induced Alfvén eigenmodes (TAEs) and energetic particle modes (EPMs), both variants of Alfvén waves whose characteristics are determined by the doubly periodic toroidal geometry and inhomogeneities of magnetic field and density.

This Letter presents the first measurement of two resonant modes excited by fast ion injection in the reversed field pinch (RFP) and characterizes observed mode frequencies and frequency scalings. Alfvén eigenmodes have been observed in many devices: tokamaks [3], spherical tokamaks [4], stellarators [5], and reversed field pinches [6,7]. Whereas TAEs arise due to the toroidal geometry of magnetic fields, EPMs are the consequence of a large fast ion population in resonance with the Alfvén continuum at a radial location [8,9]. Confinement experiments with strong ion-cyclotron-resonance heating or neutral beam injection (NBI) have been used to study EPMs [5,10]. Theoretical investigations of both types of modes have been performed extensively on tokamaks [11] and stellarators [12,13]. On

the RFP, the core magnetic field, and consequently the core parallel wave vector, are perpendicular to the field near the edge. This high-shear configuration could have interesting consequences for TAEs and EPMs, which have radial extent that can span from core to edge. Experiments in tokamaks targeted at strong magnetic shear and negative shear effects on Alfvénic instabilities have been performed in the past [14]. However, strong negative shear across the entire plasma is unique to RFPs, whose toroidal field B_t at the plasma surface vanishes or is antiparallel to the core toroidal field. Theoretical investigations of similar depth to tokamak studies have not been performed for the RFP, so the result of fast particle effects alongside high reversed shear is unknown. Additionally, magnetic reconnection during sawtooth crashes has been shown to inject energy into Alfvén modes on the RFP [7], a process with possible relation to anomalous ion heating [15]. Madison symmetric torus (MST) is in a unique position to study TAEs and EPMs in the RFP due to the recent installation of a hydrogen neutral beam injector [16].

Both EPMs and TAEs arise from modifications to the Alfvén continuum, the smoothly varying set of frequency solutions for shear Alfvén waves propagating along magnetic field lines. Their frequency is $\omega = k_{\parallel} v_A$, where $k_{\parallel} = \frac{m-nq}{r} \frac{B_{\theta}}{|B|}$, based on the cylindrical approximation where m and n are poloidal and toroidal mode numbers, r is the minor radial location, q is the safety factor, and B_{θ} is the poloidal magnetic field [17]. These solutions are strongly damped. Toroidicity introduces frequency gaps in the spectrum, within which the TAEs are discrete, undamped eigenmodes that scale with v_A . By contrast, EPMs result from frequency resonance of the characteristic frequencies (bounce, transit, or precession) of a population of fast ions. The mode expands radially from resonance with

a narrow set of radial locations in the Alfvén continuum. These modes scale with fast ion v_{\parallel} . The drive from the fast ion population must be strong enough to overcome continuum damping, resulting in a coherent mode with global extent.

The experiment was performed on MST, an axisymmetric toroidal plasma confinement device operated in the reversed field pinch configuration with a thick conducting aluminum shell [18]. The major and minor radii are $R_0 = 1.5$ m and $a = 0.5$ m, respectively. Typical experimental plasma parameters are plasma current of 0.3 MA, line-averaged electron density $n_e \approx 0.7 \times 10^{19} \text{ m}^{-3}$, n_i inferred from charge neutrality, core magnetic field $B_t = 0.3$ T, and ion temperature $T_i \approx 180$ eV. Scaling studies were done by varying parameters about these typical values. The B_t at the plasma surface is held at 0, resulting in an outer safety factor $q_a = 0$ and on-axis safety factor $q_0 = 0.21$; see Fig. 1(a). This equilibrium is chosen to minimize effects resulting from $m = 0$ resonant modes, while maintaining the RFP's characteristic feature of large, reversed magnetic shear.

NBI generates fast ions capable of exciting instabilities. Neutral hydrogen is tangentially injected at 25 keV with 1 MW of power and ionizes primarily within 10 cm of the magnetic axis [16]. The hot ion distribution function is highly sensitive to plasma parameters. For relevant experimental parameters, the trapped fraction is less than 5%.

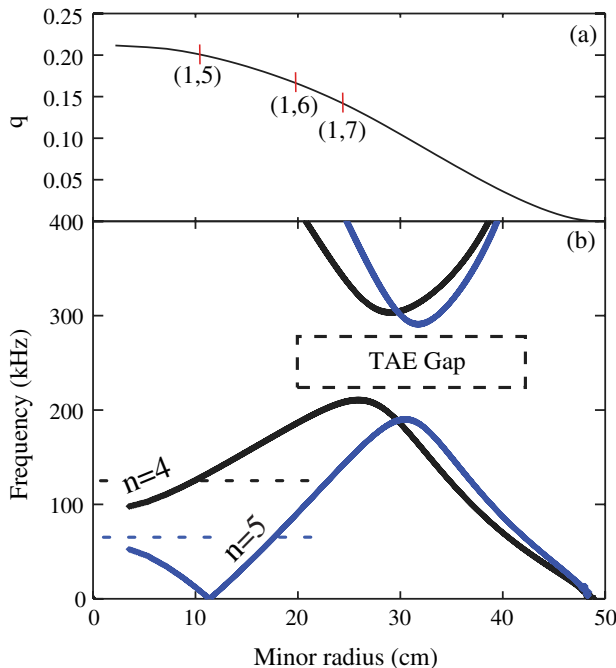


FIG. 1 (color online). (a) MST q profile calculated using MSTFIT on a typical experimental discharge, with tearing mode resonances marked. (b) The Alfvén continuum for $n = 4$ and $n = 5$ as calculated by STELLGAP. EPMS can be excited anywhere outside of the TAE gap. Observed $n = 4$ and $n = 5$ frequencies are plotted with dashed lines.

The fast ion distribution has been predicted using the NUBEAM module in the TRANSP code [19,20], and beam v_{\parallel} is plotted with v_A in Fig. 2. The fast ion density is $\approx 25\%$ of background plasma density in the core. The Alfvén speed lies within the parallel ion velocity gradient in the core of the plasma, allowing for inverse Landau damping [21]. A high degree of core localization allows for free energy to be drawn from the fast ion density gradient [14]. For these parameters, the circulating majority of ions in the core would have ion-orbital frequency

$$f_{\text{CE}} = \frac{v_{\parallel}}{2\pi R_0} \left(\frac{n}{1 + \sigma} - \frac{l}{q} \right) \quad (1)$$

as defined in Ref. [9], where n and l are toroidal and poloidal mode numbers of the fast ion perturbation, respectively, and σ is a small correction term that accounts for a shift of ion guiding centers off of the magnetic axis.

TAEs have been predicted in this configuration using the AE3D reduced-MHD eigenmode solver code and STELLGAP, its complementary code for calculating the Alfvén continuum [22]. Expected frequencies are $f_{\text{TAE}} > 200$ kHz, with mode numbers $n \geq 4$ and $m \geq 0$ and primarily $m = 0, 1$ coupling; see Fig. 1. Predicted frequencies across multiple equilibria scale with the local Alfvén speed v_A as expected. Preliminary calculations of Alfvén-acoustic continua including finite pressure and sound wave couplings have been made, indicating the presence of low frequency beta-induced Alfvén eigenmode and beta-induced Alfvén-acoustic eigenmode [23] gaps in addition to the TAE gap of Fig. 1(b). However, these frequencies are lower than the observed ranges of activity. AE3D and STELLGAP do not include fast ion effects, a condition necessary to calculate EPMS, although they will resonate at a frequency and radius near the calculated Alfvén continuum.

An array of magnetic pickup loops situated at the plasma boundary is used to analyze coherent mode activity. A toroidal array of 32 magnetic field coils, located 29°

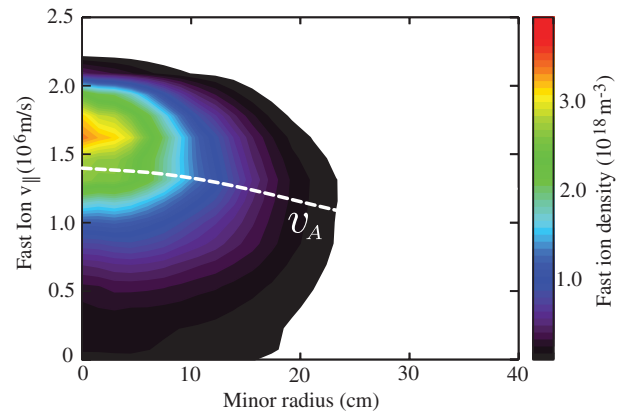


FIG. 2 (color). Fast ion density as a function of minor radius and fast ion parallel velocity after 3 ms of neutral beam injection into $n_i = 0.7 \times 10^{19} \text{ m}^{-3}$ deuterium plasma, calculated using TRANSP. Alfvén speed v_A vs radius is overplotted in white.

below the inboard horizontal midplane, is used to resolve perturbations into toroidal mode numbers. A poloidal array of eight coils resolves poloidal mode numbers. These data are digitized at 2 MHz, providing a 1 MHz Nyquist frequency. A wavelet transform of optimized shape for bursts is applied to further resolve magnetic perturbations in frequency and time. Scaling has been examined with large data sets of bursts by extracting peak frequencies at a resolution of $\Delta f/f = 4\%$.

Under varying conditions, spatially coherent magnetic bursts with several mode numbers have been observed using the magnetic arrays; see Fig. 3. The burst rate is >10 times larger for $q_a = 0$ than for plasmas with shallow reversal, e.g., $q_a \sim -0.02$, although the character of the bursts is very similar. What causes this sensitivity to field reversal remains to be determined. These bursts have toroidal mode numbers $n = 5$ and 4 and poloidal mode number $m = 1$. Mode excitation is expected in the core, but magnetic polarization at the edge is set by Ampere's law, $\nabla \times B = 0$, with $j_r = 0$ in the current-free outer region where the pickup loops reside. This fixes the ratio $\tilde{B}_r/\tilde{B}_\theta = (na)/(mR_0)$ and excludes $m = 0$ perturbations to \tilde{B}_θ . The maximum magnetic field perturbation amplitude for $n = 5$ is $\tilde{B}_\theta = 150 \mu\text{T}$ at the edge, with burst durations from 20 to 50 μs in length. The \tilde{B}_r

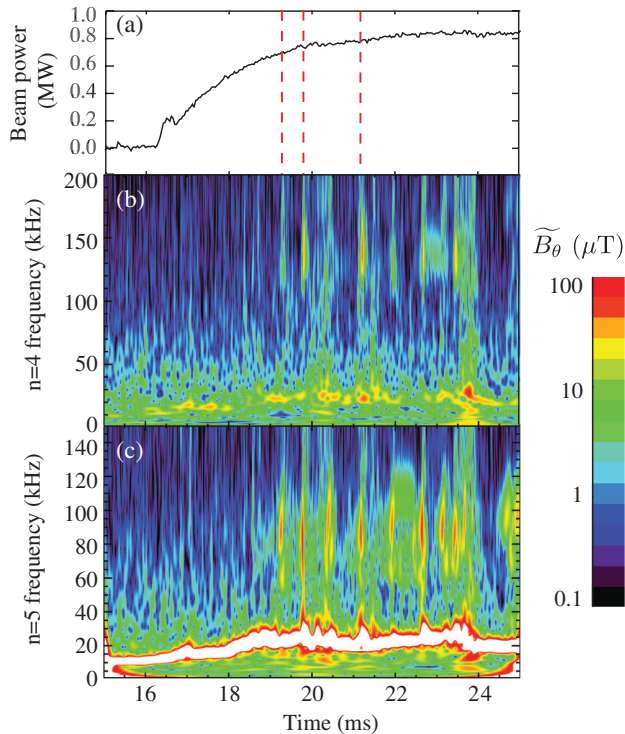


FIG. 3 (color). Beginning of neutral beam injection followed by mode turn-on. Bursts begin ≈ 2 ms after the start of beam injection, during the beam power ramp-up. (a) Dashed lines indicate burst times. (b),(c) $n = 4$ bursts immediately follow $n = 5$ bursts in time. Continuously rotating $n = 5$ tearing modes at 30 kHz are also evident in white.

component of bursts is detectable using correlation with \tilde{B}_θ , with $\tilde{B}_r/\tilde{B}_\theta \approx 1-2$, close to the expected value. After correcting for Doppler shift due to background plasma flow, the burst frequency is ≈ 65 kHz, very near the $n = 5$ continuum frequency at $r = 3$ cm and $r = 17$ cm—see Fig. 1(b)—where the fast ion distribution function has a strong radial gradient; see Fig. 2. For $n = 5$ and $m = 1$ in the plasma core, the ion-orbital frequency due to beam injection—see Eq. (1)—predicts $f_{\text{CE}} \geq 50$ kHz, near the observed value. Bursts appear only during beam injection—Figs. 3(a) and 3(c)—and bursting terminates quickly after beam turn-off, within 1–2 ms. Burst frequencies and amplitudes are reproducible under constant v_A , and subtraction of the Doppler shift results in reproducible frequency regardless of plasma rotation.

The $n = 5$, $m = 1$ mode displays scaling with beam parameters, not the background plasma Alfvén speed; it will be referred to as the EPM-like mode. Alfvén scaling is not expected for the EPM. Electron density n_e has been varied from 0.4 to $1.4 \times 10^{19} \text{ m}^{-3}$ in the core and scanned with helium, deuterium, and hydrogen gas discharges, which show weak inverse frequency scaling with mass density, $f \propto n_e^{-0.3}$; see Fig. 4(a). This unexpected scaling can be accounted for by a corresponding reduction in peak v_{\parallel} due to more rapid slowing of the fast ions as background plasma n_i is increased. Scanning core $|B|$ from 0.21 to 0.39 T (by changing the plasma current) results in no frequency change of the EPM-like mode—see Fig. 4(b)—and, thus, weak scaling with v_A ; see Fig. 5. Core plasma current may be reversed with respect to the NBI so that injected ions are counterpropagating. This has not produced evidence of mode activity, although prompt losses may bring the drive below the critical threshold for bursting. Decreasing beam power resulted in a corresponding decrease in mode amplitude. Decreasing beam ion energy from 25 to 17 keV resulted in a decrease in mode frequency with no change in toroidal or poloidal mode number; see Fig. 6. Observed frequencies are linear in v_{\parallel} , and beam energy is the only parameter varied in this case. This linear variation is in agreement with theory [9],

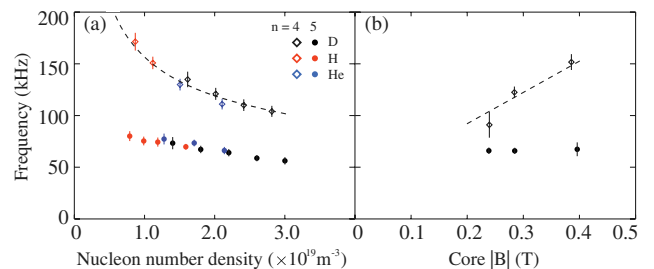


FIG. 4 (color online). Mode frequency for $n = 5$ and $n = 4$ is plotted with respect to (a) mass density ρ (expressed as nucleon number density) and (b) core $|B|$ for deuterium, hydrogen, and helium plasma ensembles. Lines with k_{\parallel} and offset calculated from v_A scaling are included.

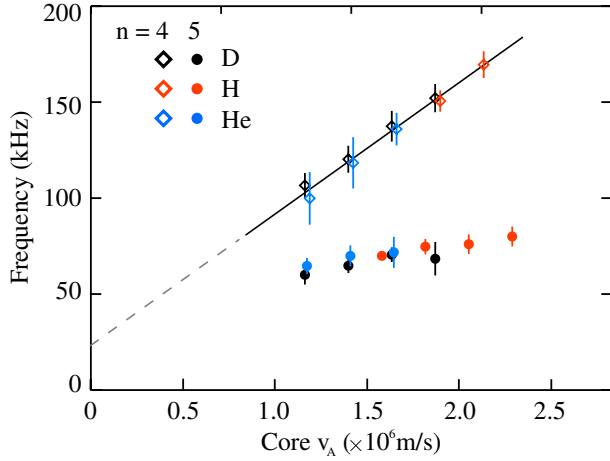


FIG. 5 (color online). Mode frequency for $n = 5$ and $n = 4$ is plotted with respect to v_A for deuterium, hydrogen, and helium plasma ensembles. A line of best fit to the $n = 4$ points is included.

suggesting that the mode is an EPM. The mode has been observed even in cases with $v_A > v_{\parallel}$, implying that excitation energy is being drawn from the radial gradient of fast ion density. Plasma rotation has a negligible effect on mode amplitude at the edge, and modes appear even in discharges without rotation.

The $n = 4$, $m = 1$ mode scales with Alfvén speed but not beam energy, and its amplitude peaks 40 μs after the EPM-like mode; see Fig. 3(b). It has been termed the AE-like mode. The growth of this mode corresponds to the damping of the EPM-like mode, indicating that energy is transferred from $n = 5$ to $n = 4$. Cross correlation of the two modes ($\tilde{b}_4 \star \tilde{b}_5$) at relevant frequencies peaks at lag $\Delta t = 40\text{--}60 \mu\text{s}$, depending on plasma parameters. The mode amplitude never exceeds the EPM-like mode

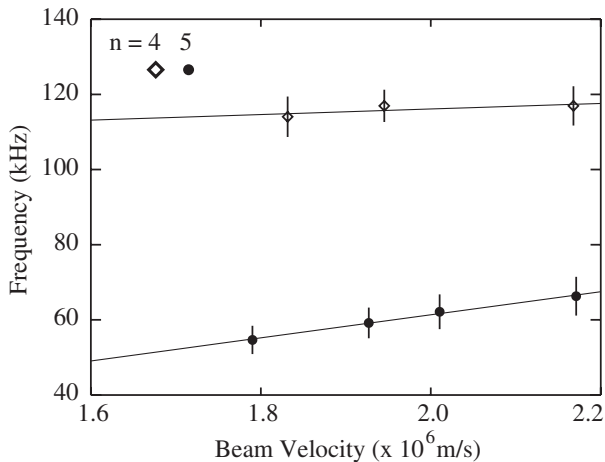


FIG. 6. Mode frequencies for the EPM-like $n = 5$ and AE-like $n = 4$ modes are plotted with respect to neutral beam velocity. A line of best fit is included and intersects the origin for the EPM-like mode case.

amplitude, and on average $\tilde{B}_{\theta,n=4} \approx 25\% \tilde{B}_{\theta,n=5}$. This behavior is characteristic of three-wave coupling observed in other machines [24]. AE-like mode frequency scales with $\rho^{-1/2}$ and scales linearly with $|B|$ —see Fig. 4—as expected for Alfvén eigenmodes; see Fig. 5. Linear correlation of the form $\omega = k_{\parallel} v_A$ for $n = 4$ yields $k_{\parallel} = 0.43 \text{ m}^{-1}$ with an offset of 25 kHz. Calculation from the Alfvén continuum yields $k_{\parallel} = 0.5 \text{ m}^{-1}$, but this number is extremely sensitive to the q profile, decreasing by 15% to the observed value with a 2.5% increase in q_0 . The offset is likely due to β effects and a shift in mode location as parameters vary. AE-like mode frequency does not scale with beam energy as seen with the EPM-like mode—see Fig. 6—and the AE-like mode bursts occur less often. It is unclear whether the two modes couple through fast ion redistribution or through magnetohydrodynamic (MHD) effects. The effect of $n = 5$ bursts on v_{\parallel} directly before the $n = 4$ burst is unknown, so inverse Landau damping cannot be ruled out as an excitation mechanism, even when equilibrium $v_A > v_{\parallel}$.

With a frequency below the Alfvén gap frequency and $f \propto v_{\parallel}$ —see Fig. 6—the $n = 5$ oscillations display behavior predicted theoretically [9] and seen on other devices [10], where they were postulated to be a resonant kinetic ballooning mode, a branch of EPM. The scaling with ion velocity is especially evident due to a weak effect from NBI on equilibrium plasma parameters. This EPM resonance has not been confirmed with computation in the RFP, but no theoretical barriers to its existence are expected. The field is ripe for computational work as existing codes are capable of handling the problem but must be adapted to the RFP geometry.

High reversed magnetic shear could have a strong effect on TAE frequency, possibly pushing it downwards and into the continuum [21]. The bursting characteristic of EPMs would then be present as the TAE crosses continuum resonances, but the mode would excite at a discrete frequency unrelated to beam energy, albeit with a drive determined by proximity to beam resonance. This mode was investigated previously and termed the resonant TAE (rTAE) [25], a type of EPM corresponding to particle drive near a downshifted TAE resonance. The $n = 4$ mode is likely an rTAE, although the capability of fast ions to excite modes within the continuum has not been accounted for in previous numerical work, so there is no computational verification of this mode in the RFP.

In summary, an EPM-like bursting mode has been detected in the RFP during beam injection. It has been detected with $n = 5$, $m = 1$ mode numbers with finite amplitude at the edge, which corresponds to Alfvén resonance in the core of the plasma. This mode scales strongly with fast ion velocity and is destabilized in plasmas with a strong radial fast ion density gradient. It appears to convert to an AE-like mode on a short time scale. Reduced-MHD predictions indicate that observed mode frequencies are below the TAE gap but have mode numbers and frequencies indicative

of an Alfvénic nature. Computation is needed to verify these modes, but experiment indicates that they resemble a resonant kinetic ballooning mode and an rTAE.

This work is supported by the U.S. DOE.

*koliner@wisc.edu

- [1] V. Mukhovatov *et al.*, *Plasma Phys. Controlled Fusion* **45**, A235 (2003).
- [2] D. Tsiklauri, *Phys. Plasmas* **18**, 092903 (2011).
- [3] M. Garcia-Munõz, H. U. Fahrbach, S. Günter, V. Igochine, M. J. Mantsinen, M. Maraschek, P. Martin, P. Piovesan, K. Sassenberg, and H. Zohm, *Phys. Rev. Lett.* **100**, 055005 (2008).
- [4] N. Gorelenkov, C. Z. Cheng, G. Y. Fu, S. Kaye, R. White, and M. V. Gorelenkova, *Phys. Plasmas* **7**, 1433 (2000).
- [5] K. Nagaoka *et al.*, *Phys. Rev. Lett.* **100**, 065005 (2008).
- [6] G. Regnoli *et al.*, *Phys. Plasmas* **12**, 042502 (2005).
- [7] S. Spagnolo, M. Zuin, F. Auremma, R. Cavazzana, E. Martines, M. Spolaore, and N. Vianello, *Nucl. Fusion* **51**, 083038 (2011).
- [8] F. Zonca and L. Chen, *Phys. Plasmas* **7**, 4600 (2000).
- [9] Y. Todo, *Phys. Plasmas* **13**, 082503 (2006).
- [10] N. Gorelenkov and W. Heidbrink, *Nucl. Fusion* **42**, 150 (2002).
- [11] F. Zonca, S. Briguglio, L. Chen, S. Dettrick, G. Fogaccia, D. Testa, and G. Vlad, *Phys. Plasmas* **9**, 4939 (2002).
- [12] D. A. Spong, R. Sanchez, and A. Weller, *Phys. Plasmas* **10**, 3217 (2003).
- [13] Y. I. Kolesnichenko, V. V. Lutsenko, H. Wobig, Y. V. Yakovenko, and O. P. Fesenyuk, *Phys. Plasmas* **8**, 491 (2001).
- [14] W. W. Heidbrink *et al.*, *Nucl. Fusion* **48**, 084001 (2008).
- [15] R. M. Magee, D. J. Den Hartog, S. T. A. Kumar, A. F. Almagri, B. E. Chapman, G. Fiksel, V. V. Mirnov, E. D. Mezonlin, and J. B. Titus, *Phys. Rev. Lett.* **107**, 065005 (2011).
- [16] J. K. Anderson *et al.*, *Trans. Fusion Sci. Technol.* **18**, 27 (2011).
- [17] A. D. Turnbull, E. J. Strait, W. W. Heidbrink, M. S. Chu, H. H. Duong, J. M. Greene, L. L. Lao, T. S. Taylor, and S. J. Thompson, *Phys. Fluids B* **5**, 2546 (1993).
- [18] R. Dexter, D. Kerst, T. Lovell, S. Prager, and J. Sprott, *Fusion Technol.* **19**, 131 (1991).
- [19] A. Pankin, D. McCune, R. Andre, G. Bateman, and A. Kritz, *Comput. Phys. Commun.* **159**, 157 (2004).
- [20] R. V. Budny, *Nucl. Fusion* **34**, 1247 (1994).
- [21] F. Zonca and L. Chen, *Phys. Plasmas* **3**, 323 (1996).
- [22] D. Spong, E. D’Azevedo, and Y. Todo, *Phys. Plasmas* **17**, 022106 (2010).
- [23] N. N. Gorelenkov, M. A. V. Zeeland, H. L. Berk, N. A. Crocker, D. Darrow, E. Fredrickson, G. Y. Fu, W. W. Heidbrink, J. Menard, and R. Nazikian, *Phys. Plasmas* **16**, 056107 (2009).
- [24] N. A. Crocker, W. A. Peebles, S. Kubota, E. D. Fredrickson, S. M. Kaye, B. P. LeBlanc, and J. E. Menard, *Phys. Rev. Lett.* **97**, 045002 (2006).
- [25] C. Z. Cheng, N. N. Gorelenkov, and C. T. Hsu, *Nucl. Fusion* **35**, 1639 (1995).